

# Quantum disordered phase near the Mott transition in the staggered-flux Hubbard model on a square lattice

Chia-Chen Chang and Richard T. Scalettar

*Department of Physics, University of California, Davis, 95616*

We investigate ground state properties of the half-filled staggered-flux Hubbard model on a square lattice. Energy gaps to charge and spin excitations and magnetic as well as dimer orders are calculated as a function of interaction strength  $U/t$  by means of constrained-path quantum Monte Carlo method. It is found that the system is a semi-metal at  $U/t \lesssim 5.6$  and a Mott insulator with long-range antiferromagnetic order at  $U/t \gtrsim 6.6$ . In the range  $5.6 \lesssim U/t \lesssim 6.6$ , the ground state is an correlated insulator where both magnetic and dimer orders are absent. Furthermore, spin excitation in the intermediate phase appears to be gapless, and the measured spin-spin correlation function exhibits power-law decaying behavior. The data suggest that the non-magnetic ground state is a possible candidate for the putative algebraic spin liquid.

PACS numbers: 71.10.Fd, 02.70.Ss

At sufficiently low temperatures, condensed matter systems have a tendency to undergo phase transitions and develop long range order which reflects broken symmetry[1]. In a two-dimensional antiferromagnet, however, Anderson recognized that the system could have a ground state that avoids all spontaneous symmetry-breaking and does not have magnetic order even at zero temperature[2]. Anderson's discovery, in conjunction with many subsequent theoretical investigations, uncovered a new class of matter, named spin liquids, that go beyond Landau's paradigm. Most notably, in contrast to conventional symmetry-breaking, spin liquids possess topological orders that cannot be characterized by local order parameters and carry fractionalized excitations[3].

Model Hamiltonians have played an important role in realizing such exotic spin liquid states[4, 5]. Evidence of spin liquid phases has been found in the spin 1/2 Heisenberg model on triangular lattices[6], square lattices with frustration[7–9], and kagome lattices[10]. In these geometrically frustrated systems[11], antiferromagnetic (AF) orders are suppressed by strong quantum fluctuations. In addition to spin systems, there is also progress using the Hubbard model which contains spin and charge degrees of freedom. Spin liquid ground states have been identified in the model on anisotropic triangular lattices[12] and on bipartite honeycomb lattices[13].

In this paper, we examine ground state properties of the half-filled staggered-flux Hubbard model (sfHM) on a square lattice. As will be seen later, low energy physics in the sfHM is described by Dirac fermions, similar to that found in the Hubbard model on honeycomb lattices[13]. The model is defined by the Hamiltonian

$$H = - \sum_{\langle ij \rangle, \sigma} (t_{ij} c_{i\sigma}^\dagger c_{j\sigma} + t_{ji} c_{j\sigma}^\dagger c_{i\sigma}) + U \sum_{\mathbf{i}} \left( n_{i\uparrow} - \frac{1}{2} \right) \left( n_{i\downarrow} - \frac{1}{2} \right), \quad (1)$$

where  $t_{ij} = t e^{i\theta_{ij}}$  is the nearest-neighbor hopping and we

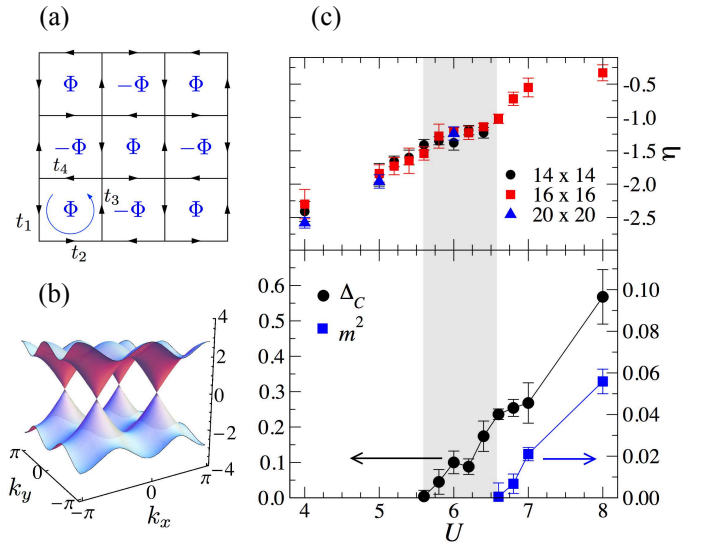


FIG. 1. (a) Arrangement of hopping amplitudes on a square lattice. The phase  $\Phi = \pi$  is distributed equally so that  $t_1 = t_2 = t_3 = t_4 = e^{i\Phi/4}$ . (b) Band structure of the tight-binding Hamiltonian. (c) Top panel: power law exponent  $\eta$  extracted from fits to staggered spin-spin correlation functions. Bottom panel: thermodynamic limit charge gap  $\Delta_C$  and magnetic moment  $m^2$  (see text for definition). The shaded region indicates the non-magnetic insulating phase.

set  $t = 1$  throughout this work. The operator  $c_{i\sigma}$  ( $c_{i\sigma}$ ) creates (annihilates) an electron with spin  $\sigma = \uparrow, \downarrow$  at site  $\mathbf{i}$  on a lattice of size  $N = L \times L$ .  $U > 0$  is the onsite Coulomb repulsion. We work in the canonical ensemble.

An electron gains a phase  $\Phi = \sum_{\square} \theta_{ij}$  when it hops around a plaquette of the square lattice.  $\Phi = 0$  corresponds to the original Hubbard model. We focus on the case  $\Phi = \pi$  in the present study. There is a gauge freedom in choosing  $\theta_{ij}$ . Here we distribute the phase

$\Phi$  equally over all bonds around a plaquette and arrange the hoppings according to Fig. 1(a). This leads to a lattice with plaquettes threaded alternatively by flux  $\Phi$  and  $-\Phi$ . At  $U = 0$ , the energy spectrum is  $\epsilon_{\mathbf{k}} = \pm 2\sqrt{\cos^2 k_x + \cos^2 k_y}$ . The two energy bands meet at the Fermi surface  $\epsilon_{\mathbf{k}} = 0$  located at nodal points  $\mathbf{k}_0 = (\pm\pi/2, \pm\pi/2)$ , as shown in Fig. 1(b). Close to the four nodal points the energy depends linearly on  $\mathbf{k}$ , which is similar to the massless Dirac spectrum found on the honeycomb lattice.

Our key result is that an intermediate non-magnetic insulating ground state is identified between the semi-metal phase at weak interaction strengths and the AF Mott insulator at strong couplings where the hopping terms become irrelevant. The calculated dimer correlation function shows that columnar valence bond order is also absent in the intermediate phase. These results seem to indicate that the non-magnetic insulating phase is a candidate for the putative algebraic spin liquid ground state. Therefore, our work suggests recent progress in optical lattice experiments[14] might provide a promising way of simulating the model, and observing this novel state of matter.

The sfHM is solved numerically by means of the constrained-path quantum Monte Carlo method[15]. Details of the method are described in the supplemental materials. We begin with the results for the charge excitation gap. In the canonical ensemble, the charge gap at half-filling can be defined as[16]

$$\Delta_C(L) = \frac{1}{2} \left[ E_g \left( \frac{N}{2} - 1, \frac{N}{2} - 1 \right) - E_g \left( \frac{N}{2}, \frac{N}{2} \right) \right], \quad (2)$$

which is the energy cost of removing a pair of electrons from the half-filled ground state while keeping the system in the  $S_{tot}^z = 0$  sector. We measure  $\Delta_C(L)$  as a function of interaction strength  $U$  on lattices with linear dimension up to  $L = 14$ . As shown in the inset of Fig. 2(a), the charge gap increases with  $U$  on finite lattices. To pinpoint the critical interaction strength where the system turns into an insulator, we extrapolate  $\Delta_C(L)$  at fixed  $U$  to the thermodynamic limit  $L \rightarrow \infty$  using second order polynomials in  $L^{-1}$ . The results, shown in the inset of Fig. 2(a), indicate that the system is gapped for  $U \gtrsim 5.6$ .

In addition to the charge excitation gap, AF long-range order is another essential feature characterizing a Mott insulator. To investigate whether there is any AF order in the ground state, we calculate the spin structure factor at the Néel wave vector  $\mathbf{q}_{AF} = (\pi, \pi)$

$$S(\mathbf{q}_{AF}, L) = \sum_{\mathbf{r}} e^{i\mathbf{q}_{AF} \cdot \mathbf{r}} \langle S_{\mathbf{r}}^x S_0^x + S_{\mathbf{r}}^y S_0^y + S_{\mathbf{r}}^z S_0^z \rangle, \quad (3)$$

where  $S_{\mathbf{r}}^{\delta}$  is the spin operator along the  $\delta$ -direction ( $\delta = x, y, z$ ), and  $\langle S_{\mathbf{r}}^{\delta} S_0^{\delta} \rangle$  is the equal-time spin-spin correlation function. Defining  $m^2(L) = S(\mathbf{q}_{AF}, L)/L^2$ , a magnetically ordered phase is singled by a finite  $m^2(L)$  in

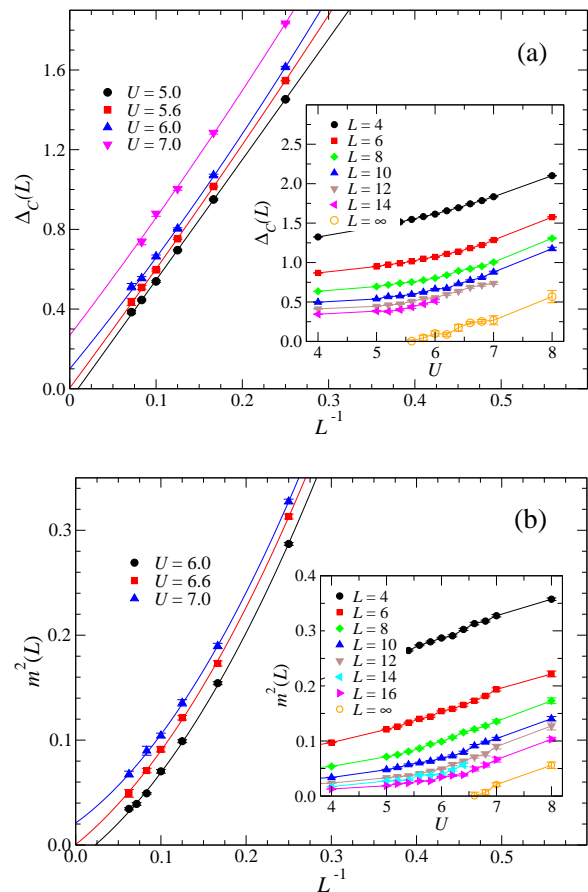


FIG. 2. (a) Extrapolation of the charge gap  $\Delta_C(L)$ . Solid lines represent second-order polynomial fits to the QMC data. Inset shows the charge gap  $\Delta_C(L)$  as a function of  $U$  obtained for  $L = 4, 6, 8, 10, 12, 14$ , and extrapolated (empty circle) values. Lines are guides to the eyes. (b) Finite size extrapolation of the spin structure factor  $m^2(L)$ . Solid lines are second-order polynomial fits to the QMC data. Inset:  $m^2(L)$  versus  $U$  on finite lattices and extrapolated (empty circle) values. Lines are guide to the eyes.

the thermodynamic limit. The inset of Fig. 2(b) shows the results of  $m^2(L)$  as a function of  $U$  on finite lattices. We use second-order polynomials in  $L^{-1}$  to fit the QMC data and extract the value of  $m^2(L)$  in the  $L \rightarrow \infty$  limit. It can be seen from the inset of Fig. 2(b) that AF order kicks in at  $U \gtrsim 6.6$ , below which the system is in a paramagnetic phase.

Our analysis of charge gap and magnetic order above suggests that the ground state of the sfHM is a semi-metal at  $U \lesssim 5.6$ , and becomes a Mott insulator with long-range AF order at  $U \gtrsim 6.6$ . Therefore, unlike the original half-filled Hubbard model which enters the Mott phase at arbitrarily small  $U$ , the sfHM has a finite Mott transition point. This finding is consistent with a previous finite-temperature determinant quantum Monte Carlo work[17] which reports that the critical point of Mott transition in the staggered-flux model lies in the

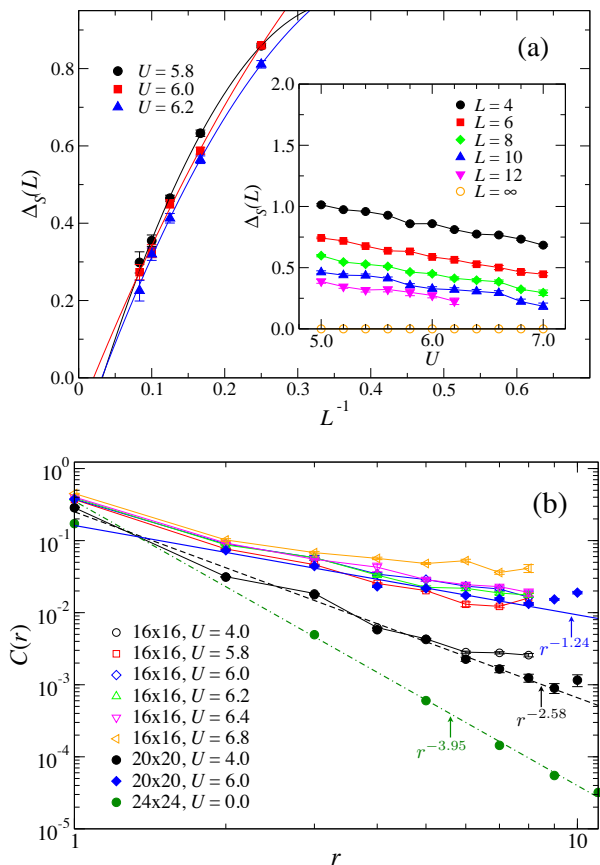


FIG. 3. (a) Finite size extrapolation of the spin gap  $\Delta_S(L)$ . Solid lines are second-order polynomial fits to the Monte Carlo data. The inset illustrates  $\Delta_S(L)$  and its extrapolated value. Lines are guide to the eyes. (b) Long-range behavior of the staggered spin-spin correlation function  $C(\mathbf{r}) = (-1)^r \langle S_r^x S_0^x + S_r^y S_0^y + S_r^z S_0^z \rangle$  obtained on  $L = 16, 20$ , and  $24$  ( $U = 0$  only). Straight lines are representative power-law fits to the data: Green (dot-dashed) line:  $L = 24$  at  $U = 0$ , black (dashed) line:  $L = 20$  at  $U = 4$ , and purple (solid) line:  $L = 20$  at  $U = 6$ .

range  $4 \leq U \leq 8$ . Moreover, our results indicate that in the region  $5.6 \lesssim U \lesssim 6.6$  there is an intermediate phase that is neither a semi-metal nor a Mott insulator.

The absence of AF order in the intermediate phase indicates that the ground state is dominated by short-range spin correlations. At large distances, the spin correlation function could either decay exponentially or follow a power-law. To study the nature of the non-magnetic insulating phase, we first calculate the spin excitation gap. Following Ref. [18], we write the spin gap at half-filling as

$$\Delta_S(L) = E_g \left( \frac{N}{2} + 1, \frac{N}{2} - 1 \right) - E_g \left( \frac{N}{2}, \frac{N}{2} \right), \quad (4)$$

which measures the energy cost of flipping an electron from spin-down to spin-up. Based on confinement arguments, a gapped spin excitation implies a finite correlation length, leading to an exponentially decaying spin-

spin correlation. On the other hand, the correlation function would be described by a power-law if the spin excitation is gapless. We compute  $\Delta_S(L)$  as a function of  $U$  on finite lattices. The spin gap results are shown in the inset of Fig. 3(a) for  $5 \leq U \leq 7$ . The data at a given  $U$  is then extrapolated to  $L \rightarrow \infty$  using a second-order polynomial in  $L^{-1}$  to extract the spin gap in the thermodynamic limit. Typical behavior of the fits is plotted in Fig. 3(a). As expected, the extrapolated spin gap remains zero in the gapless semi-metal phase ( $U \lesssim 5.6$ ) and in the Mott phase ( $U \gtrsim 6.6$ ) due to the presence of gapless spin wave excitations. More importantly,  $\Delta_S(L)$  also shows gapless behavior in the region  $5.6 \lesssim U \lesssim 6.6$ , implying that the spin-spin correlation should follow a power-law at large distances.

To support this observation, we plot in Fig. 3(b) the staggered spin-spin correlation function along the  $x$ -axis. It appears that  $C(\mathbf{r})$  indeed decays algebraically at large separations. Moreover, the correlation function decays more slowly with increasing  $U$ , and starts showing saturation in the Mott phase  $U \gtrsim 6.6$ . In order to quantify the long-range behavior of  $C(\mathbf{r})$ , we fit the staggered spin correlation function to a power law  $\alpha|\mathbf{r}|^\eta$  for  $|\mathbf{r}| \geq 2$ , where  $\alpha$  and  $\eta$  are two fitting parameters. At  $U = 0$ , it is known that  $C(\mathbf{r})$  decays as  $|\mathbf{r}|^{-4}$ [19]. This is also demonstrated in Fig. 3(b): the fitted exponent of  $C(\mathbf{r})$  for free fermions on a half-filled  $24 \times 24$  is  $\eta = -3.95 \pm 0.13$ . The exponent  $\eta$  as a function of  $U$  extracted from several half-filled lattices is plotted in the top panel of Fig. 1(c). It can be seen from the figure that  $\eta$  immediately increases with  $U$  from its non-interacting value due to the effect of interaction. Although the data is quite scattered, the figure suggests that the exponent  $\eta$  increases slowly with  $U$  in the region  $5.6 \lesssim U \lesssim 6.6$ .

Next we consider other order parameters proposed in Ref. [19]. The simplest scenario is the columnar valence bond solid (VBS) which breaks translational symmetry. The VBS order can be probed by measuring the dimer structure factor

$$D_{\delta\delta}(\mathbf{q}, L) = \frac{1}{N} \sum_{\mathbf{r}} e^{i\mathbf{q}\cdot\mathbf{r}} C_{\delta\delta}^z(\mathbf{r}), \quad (5)$$

where  $C_{\delta\delta}^z(\mathbf{r})$  is the  $z$ -component equal-time dimer-dimer correlation function for singlet bonds along the  $\delta$ -direction ( $\delta = x, y$ )

$$C_{\delta\delta}^z(\mathbf{r}) = \langle S_{\mathbf{r}+\delta}^z S_{\mathbf{r}}^z S_{\delta}^z S_0^z \rangle - \langle S_{\delta}^z S_0^z \rangle^2. \quad (6)$$

In the columnar VBS state, dimers line up coherently. Therefore  $D_{\delta\delta}(\mathbf{q}, L)$  would pick up a characteristic momentum at  $\mathbf{k}_{xx} = (\pi, 0)$  or  $\mathbf{k}_{yy} = (0, \pi)$  for  $\delta = x$  or  $y$  depending on the orientation of the bonds. Indeed  $D_{\delta\delta}(\mathbf{q}, L)$  peaks at  $\mathbf{k}_{\delta\delta}$  in our finite size simulations, as shown in the supplemental materials. To extract the VBS order in the thermodynamic limit, we calculate  $d_{\delta\delta}^2(L) = D_{\delta\delta}(\mathbf{k}_{\delta\delta})/N$  and extrapolate to the  $L \rightarrow \infty$

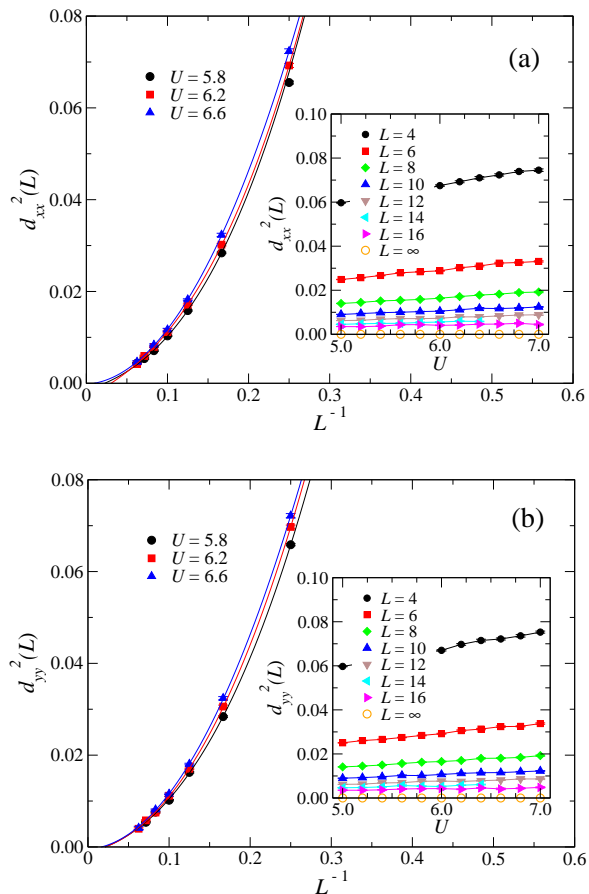


FIG. 4. Thermodynamic limit extrapolation of the columnar VBS order. In both figures, solid lines are three representative third-order polynomial fits to the Monte Carlo data. Insets show the normalized dimer structure for single bonds in  $x$  or  $y$  directions on finite size lattices. Lines are guide to the eyes. The extrapolated value in the thermodynamic limit is indicated by orange (empty) circles in the insets.

limit. As shown in Fig. 4(a) and (b), both quantities vanish in the thermodynamic limit, implying the absence of columnar VBS order in the intermediate phase.

A commonly adopted definition of a spin liquid is that it is a non-magnetic Mott insulator in which neither spin nor lattice symmetry is broken. Based on this definition, our numerical data presented in this work seems to suggest an *algebraic* spin liquid ground state in the half-filled sfHM. However, the most unambiguous evidence of a spin liquid is its fractionalized excitation[20]. Due to the nature of our method, we are not able to directly measure quantum properties of excited states. In terms of the method, we note that although the half-filled staggered-flux model does not have the fermion sign problem, we deliberately keep the constrained-path approximation and calculate the ground state properties at half-filling. Our benchmark data shows that the error appears to be small when compared with exact answers, as shown by the benchmark data in supplemental materials.

However, it is possible that the systematic error grows with  $L$ . A recent exact QMC method, linearized auxiliary fields Monte Carlo technique, reports that the half-filled ground state energy at  $U = 4$  is  $-0.85996(5)$ [21] per site in the thermodynamic limit. Our method, after boundary condition averaging, gives  $-0.8559(4)$ [22], corresponding to a 0.47% error. By including this systematic error, we estimate that the lower critical point where charge gap opens would be pushed to  $U \sim 5.4 \pm 0.1$ . In observable results such as correlation functions, extensive tests[15, 23] show that our systematic error is small even at half-filling[23] and does not affect the physics of the numerical solutions.

To summarize, we have studied ground state properties in the half-filled staggered-flux Hubbard model on a square lattice. Charge and spin excitation gaps as well as spin and dimer orders are extracted by means of the constrained-path quantum Monte Carlo method. The system is found to be a semi-metal at  $U \lesssim 5.6$  and an AF Mott insulator at  $U \gtrsim 6.6$ . In the region  $5.6 \lesssim U \lesssim 6.6$ , our data suggests that both AF and VBS orders are absent in the ground state. Spin excitation in this region is gapless, a result that is consistent with the calculated staggered spin-spin correlation function which shows power-law decaying behavior at large distances.

We thank Professors Rajiv R. P. Singh and Shiwei Zhang for helpful comments. C.C. would like to thank Professor Hong Yao for illuminating discussions. This research was supported by the DOE SciDAC (Grant No. DOE-DE-FC0206ER25793) and NSF PIF (Grant No. NSF-PHY-1005503) Programs. Computations were performed on Kraken at the National Institute for Computational Sciences.

- 
- [1] L. Landau, Phys. Z. Sowjun. **11**, 26 (1937).
  - [2] P. Anderson, Mat. Res. Bull. **8**, 153 (1973).
  - [3] X.-G. Wen, Phys. Rev. B **65**, 165113 (2002).
  - [4] J. Marston and C. Zeng, J. App. Phys. **69**, 5962 (1991).
  - [5] S. Sachdev, Phys. Rev. B **45**, 12377 (1992).
  - [6] S. Yunoki and S. Sorella, Phys. Rev. B **74** (2006).
  - [7] A. Sandvik, Phys. Rev. Lett. **98** (2007).
  - [8] H.-C. Jiang, H. Yao, and L. Balents, arXiv:1112.2241 (2011).
  - [9] L. Wang, Z.-C. Gu, F. Verstraete, and X.-G. Wen, arXiv:1112.3331 (2011).
  - [10] S. Yan, D. A. Huse, and S. R. White, Science **332**, 1173 (2011).
  - [11] L. Balents, Nature **464**, 199 (2010).
  - [12] H. Morita, S. Watanabe, and M. Imada, J. Phys. Soc. Jpn. **71**, 2109 (2002).
  - [13] Z. Meng, T. Lang, S. Wessel, F. Assaad, and A. Muramatsu, Nature **464**, 847 (2010).
  - [14] M. Aidelsburger, M. Atala, S. Nascimbène, S. Trotzky, Y. A. Chen, and I. Bloch, Phys. Rev. Lett. **107**, 255301 (2011).
  - [15] S. Zhang, J. Carlson, and J. Gubernatis, Phys. Rev.

- Lett. **74**, 3652 (1995); Phys. Rev. B **55**, 7464 (1997).
- [16] N. Furukawa and M. Imada, J. Phys. Soc. Jpn. **61**, 3331 (1992).
- [17] Y. Otsuka and Y. Hatsugai, Phys. Rev. B **65**, 073101 (2002).
- [18] R. Noack, S. White, and D. Scalapino, Europhys. Lett. **30**, 163 (1995).
- [19] M. Hermele, T. Senthil, and M. P. A. Fisher, Phys. Rev. B **72** (2005).
- [20] G. Misguich, in *Introduction to Frustrated Magnetism*, edited by C. Lacroix, F. Mila, and P. Mendels (Springer, 2010) p. 407.
- [21] S. Sorella, Phys. Rev. B **84**, 241110(R) (2011).
- [22] C.-C. Chang and S. Zhang, Phys. Rev. B **78**, 165101 (2008).
- [23] S. Zhang, J. Carlson, and J. Gubernatis, Phys. Rev. Lett. **78**, 4486 (1997).

# Supplemental Material for “Quantum disordered phase near the Mott transition in the staggered-flux Hubbard model on a square lattice”

Chia-Chen Chang and Richard T. Scalettar  
*Department of Physics, University of California, Davis, 95616*

## METHOD AND BENCHMARKS

The square lattice staggered-flux Hubbard model (sfHM) is solved numerically by using the ground state constrained-path quantum Monte Carlo (CPQMC) method[1]. The CPQMC method projects the many-body ground state wave function  $|\Psi_0\rangle$  from a trial state  $|\Psi_T\rangle$ , assuming  $\langle\Psi_T|\Psi_0\rangle \neq 0$ , by successively applying an imaginary-time propagator  $e^{-\Delta\tau H}$  to  $|\Psi_T\rangle$  with  $\Delta\tau$  being the imaginary-time step. The propagator is decomposed according to the second order Trotter-Suzuki formula[2]. The two-body part of the resulting operator is then transformed into one-body projectors using a spin-decomposed Hubbard-Stratonovich (HS) transformation[3]. Apart from systematic errors due to Trotter break-up, we arrive at a formally exact expression  $e^{-\Delta\tau H} = \sum_{\{\mathbf{x}\}} P(\{\mathbf{x}\})B(\{\mathbf{x}\})$ , where  $\{\mathbf{x}\}$  is a collection of  $N$  Ising-like HS variables,  $P(\{\mathbf{x}\})$  is their probability distribution, and  $B(\{\mathbf{x}\})$  is a one-body projector. The projection is then realized by importance-sampled open-ended random walks with non-orthogonal Slater determinants (SDs), where the projectors  $B(\{\mathbf{x}\})$  propagate one SD into another.

Away from half-filling (one electron per lattice site), the fermion sign problem is controlled by the constrained-path approximation[1]. The ground state wave function obtained by the CPQMC method is written as  $|\Psi_0^c\rangle = \sum_{\phi} w(\phi)|\phi\rangle$ , where  $|\phi\rangle$  are SDs sampled by the QMC,  $w(\phi)$  are weight factors dictated by the distribution of  $|\phi\rangle$ . Since the Schrödinger equation is linear,  $|\Psi_0^c\rangle$  and  $-|\Psi_0^c\rangle$  are two degenerate solutions which can be both sampled in a random walk. The appearance of the two sets with opposite signs in the Monte Carlo samples is the origin of the exponential sign decay. To control the problem, we restrict the walkers such that at each step of projection the condition  $\langle\Psi_T|\phi\rangle > 0$  is fulfilled.

After the random walk has equilibrated, expectation values can be computed from  $|\Psi_0^c\rangle$ . For example, the ground state energy is evaluated using a mixed estimator

$$E_g = \frac{\langle\Psi_T|H|\Psi_0^c\rangle}{\langle\Psi_T|\Psi_0^c\rangle}, \quad (1)$$

where  $H$  is the Hamiltonian. For observables that does not commute with  $H$ , we use a scheme called back-propagation (BP)[1] which is similar to the forward-walking technique in the Green’s Function Monte Carlo method[4]. Throughout this work, we use free electron wave functions as our  $|\Psi_T\rangle$ . A very small amount of

anisotropy ( $\delta\Phi = 0.002\Phi$ ) is added to the total flux per plaquette  $\Phi = \pi$  in order to lift the two-fold degeneracy in the finite size single-particle spectrum. We also average our results over boundary conditions so that finite size effects can be minimized.

To access the accuracy of our method, we compare the energy of a  $4 \times 4$  Hubbard cluster at  $U = 4$  and  $\Phi = 0$ . Let  $E_g(N_\uparrow, N_\downarrow)$  denote the energy of the system with  $N_\uparrow$  ( $N_\downarrow$ ) spin-up (-down) electrons. The exact energy per site is  $E_g(7, 7)/N = -0.9831$ [5], where  $N = L \times L$  is the number of lattice sites of an  $L \times L$  square lattice. After correcting the Trotter error, the CPQMC method gives  $-0.9821(6)$ , corresponding to an error of 0.1%. At half-filling, the exact energy is  $E_g(8, 8)/N = -0.8513$ [5]. The CPQMC energy obtained *with* constrained-path approximation is  $-0.8491(2)$ , which is within 0.26% of the exact energy. Comparisons of other observables, such as spin-spin correlation function, computed using the BP scheme can be found in Ref. 1, and 6.

## DIMER CORRELATION AND STRUCTURE FACTOR

The dimer-dimer correlation function examined in this work is defined as

$$C_{\delta\delta}^z(\mathbf{r}) = \langle S_{\mathbf{r}+\delta}^z S_{\mathbf{r}}^z S_{\delta}^z S_0^z \rangle - \langle S_{\delta}^z S_0^z \rangle^2, \quad (2)$$

where  $S_{\mathbf{r}}^z$  is the  $z$ -component spin 1/2 operator at site  $\mathbf{r}$ .  $\delta = x$  or  $y$  denotes the orientation of singlet bonds. Typical behavior of the dimer-dimer correlation function is shown in Fig. 1. for a  $16 \times 16$  lattice at half-filling with interaction strength  $U = 6.8$ .

We are also interested in the dimer structure factor. This quantity is defined as

$$D_{\delta\delta}(\mathbf{q}, L) = \frac{1}{N} \sum_{\mathbf{r}} e^{i\mathbf{q}\cdot\mathbf{r}} C_{\delta\delta}^z(\mathbf{r}). \quad (3)$$

Fig. 2 illustrates the dimer structure factor obtained for a  $L = 16$  lattice at  $U = 6.8$ . In this example,  $D_{xx}(\mathbf{q}, 16)$  peaks at the dimer characteristic wave vector  $\mathbf{q} = (\pi, 0)$ , indicating a weak dimer order on a finite lattice. To determine whether the ground state is dimerized, we extrapolate  $D_{\delta\delta}(\mathbf{q}, L)$  at  $\mathbf{q} = (\pi, 0)$  or  $(0, \pi)$  to the  $L \rightarrow \infty$  limit, and extract its bulk value. The results are shown in the main text.

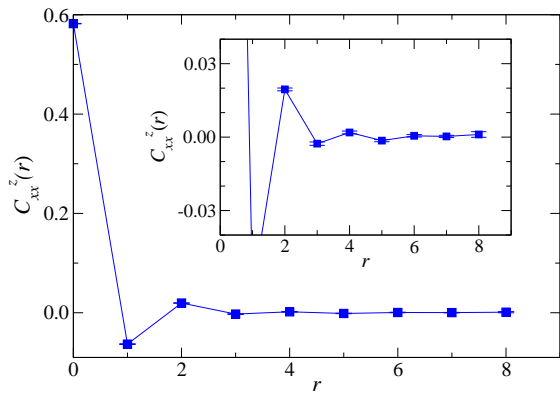


FIG. 1. Dimer-dimer correlation function  $C_{xx}^z(\mathbf{r})$  obtained on a  $16 \times 16$  lattice at  $U = 6.8$ . The correlation function is plotted along the  $x$ -axis. The inset shows the behavior of  $C_{xx}^z(\mathbf{r})$  for  $|\mathbf{r}| \geq 2$ .

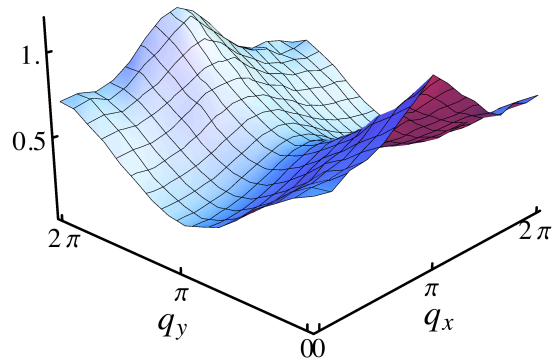


FIG. 2. Dimer structure factor  $D_{xx}(\mathbf{q}, L)$  obtained on a  $L = 16$  square lattice at half-filling and  $U = 6.8$ .

- 
- [1] S. Zhang, J. Carlson, and J. Gubernatis, Phys. Rev. Lett. **74**, 3652 (1995); Phys. Rev. B **55**, 7464 (1997).
  - [2] M. Suzuki, Comm. Math. Phys. **51**, 183 (1976).
  - [3] J. Hirsch, Phys. Rev. B **28**, 4059 (1983).
  - [4] M. Kalos, J. Comput. Phys. **2**, 257 (1967).
  - [5] E. Dagotto, A. Moreo, F. Ortolani, D. Poilblanc, and J. Riera, Phys. Rev. B **45** (1992).
  - [6] S. Zhang, J. Carlson, and J. Gubernatis, Phys. Rev. Lett. **78**, 4486 (1997).